Cell Reports
Article

PKA Phosphorylates the ATPase Inhibitory Factor 1 and Inactivates Its Capacity to Bind and Inhibit the Mitochondrial H^+-ATP Synthase

Javier García-Bermúdez,[1] María Sánchez-Aragó,[1] Beatriz Soldevilla,[1] Araceli del Arco,[1,2] Cristina Nuevo-Tapioles,[1] and José M. Cuezva[1,*]
[1]Departamento de Biología Molecular, Centro de Biología Molecular Severo Ochoa, Consejo Superior de Investigaciones Científicas-Universidad Autónoma de Madrid (CSIC-UAM), Centro de Investigación Biomédica en Red de Enfermedades Raras CIBERER-ISCIII, Instituto de Investigación Hospital 12 de Octubre, Universidad Autónoma de Madrid, 28049 Madrid, Spain
[2]Área de Bioquímica, Universidad de Castilla la Mancha, 45071 Toledo, Spain
*Correspondence: jmcuezva@cbm.csic.es
http://dx.doi.org/10.1016/j.celrep.2015.08.052

SUMMARY

The mitochondrial H^+-ATP synthase synthesizes most of cellular ATP requirements by oxidative phosphorylation (OXPHOS). The ATPase Inhibitory Factor 1 (IF1) is known to inhibit the hydrolase activity of the H^+-ATP synthase in situations that compromise OXPHOS. Herein, we demonstrate that phosphorylation of S39 in IF1 by mitochondrial protein kinase A abolishes its capacity to bind the H^+-ATP synthase. Only dephosphorylated IF1 binds and inhibits both the hydrolase and synthase activities of the enzyme. The phosphorylation status of IF1 regulates the flux of aerobic glycolysis and ATP production through OXPHOS in hypoxia and during the cell cycle. Dephosphorylated IF1 is present in human carcinomas. Remarkably, mouse heart contains a large fraction of dephosphorylated IF1 that becomes phosphorylated and inactivated upon in vivo β-adrenergic stimulation. Overall, we demonstrate the essential function of the phosphorylation of IF1 in regulating energy metabolism and speculate that dephosho-IF1 might play a role in signaling mitohormesis.

INTRODUCTION

The mitochondrial H^+-ATP synthase (Walker, 2013) synthesizes most of the ATP that is needed to sustain cellular activity in normal differentiated cells. This protein complex also participates in the execution of cell death (Sánchez-Aragó et al., 2013a) and in shaping mitochondrial ultrastructure (Paumard et al., 2002). In mitochondria, futile ATP hydrolysis by the H^+-ATP synthase is inhibited by the ATPase Inhibitory Factor 1 (IF1) that reversibly binds to the enzyme (Walker, 2013). The structure of the inhibited F1-ATPase complex with bound IF1 in the presence of ATP has been solved (Bason et al., 2014; Cabezón et al., 2003). Residues 1–37 in the mature IF1 stabilize the binding of the inhibitor to the αβ-interface in the F1-ATPase domain, blocking rotary catalysis (Cabezón et al., 2003). The expression of IF1 varies greatly between different normal human tissues and is highly overexpressed in some prevalent human carcinomas (Sánchez-Aragó et al., 2013b; Sánchez-Cenizo et al., 2010). The physiological function ascribed to IF1 is to inhibit the hydrolase activity of the H^+-ATP synthase when mitochondria becomes de-energized, such as in hypoxic cells (Campanella et al., 2008; Gledhill et al., 2007). However, data obtained in cancer (Formentini et al., 2012; Sánchez-Aragó et al., 2013b; Sánchez-Cenizo et al., 2010) and in stem cells (Sánchez-Aragó et al., 2013c), as well as in mouse models overexpressing an active IF1 in neurons (Formentini et al., 2014), support that, in the in vivo context, IF1 also inhibits the synthase activity of the H^+-ATP synthase. Moreover, the IF1-mediated inhibition of the enzyme has been shown to trigger a mild reactive oxygen species (ROS) signal that promotes metabolic reprogramming and nuclear preconditioning aimed at preventing cell death (Formentini et al., 2012; Sánchez-Aragó et al., 2013b), two events that favor neuroprotection in vivo after challenging the brain of transgenic IF1-expressing mice with an excitotoxic insult (Formentini et al., 2014). In line with these findings, silencing of IF1 has been shown to ameliorate severe mitochondrial respiratory chain dysfunctions (Chen et al., 2014).

Despite the main role of IF1 in pathophysiology, the mechanisms that regulate its activity in vivo are basically unknown. Previous phosphoproteomic analyses have reported that IF1 is phosphorylated in S39 in skeletal muscle (Zhao et al., 2011) and cancer cell lines (Sharma et al., 2014; Zhou et al., 2013). The phosphorylation of human IF1 in S63 has also been reported (Christensen et al., 2010; Zhou et al., 2013). In this study, we show that activation of PKA phosphorylates IF1 and that phosphorylation of S39 in IF1 interferes with its ability to interact with the H^+-ATP synthase. Remarkably, phosphorylation of IF1 affects both the synthetic and hydrolytic activities of the enzyme and contributes to in vivo metabolic reprogramming for adaptation to different physiological contexts.

RESULTS

IF1 Is Phosphorylated in Some Human Cancer Cell Lines

Protein extracts of colon (HCT116), cervix (HeLa), breast (BT549), lung (HOP62), and ovarian (OVCAR8) cancer cell lines

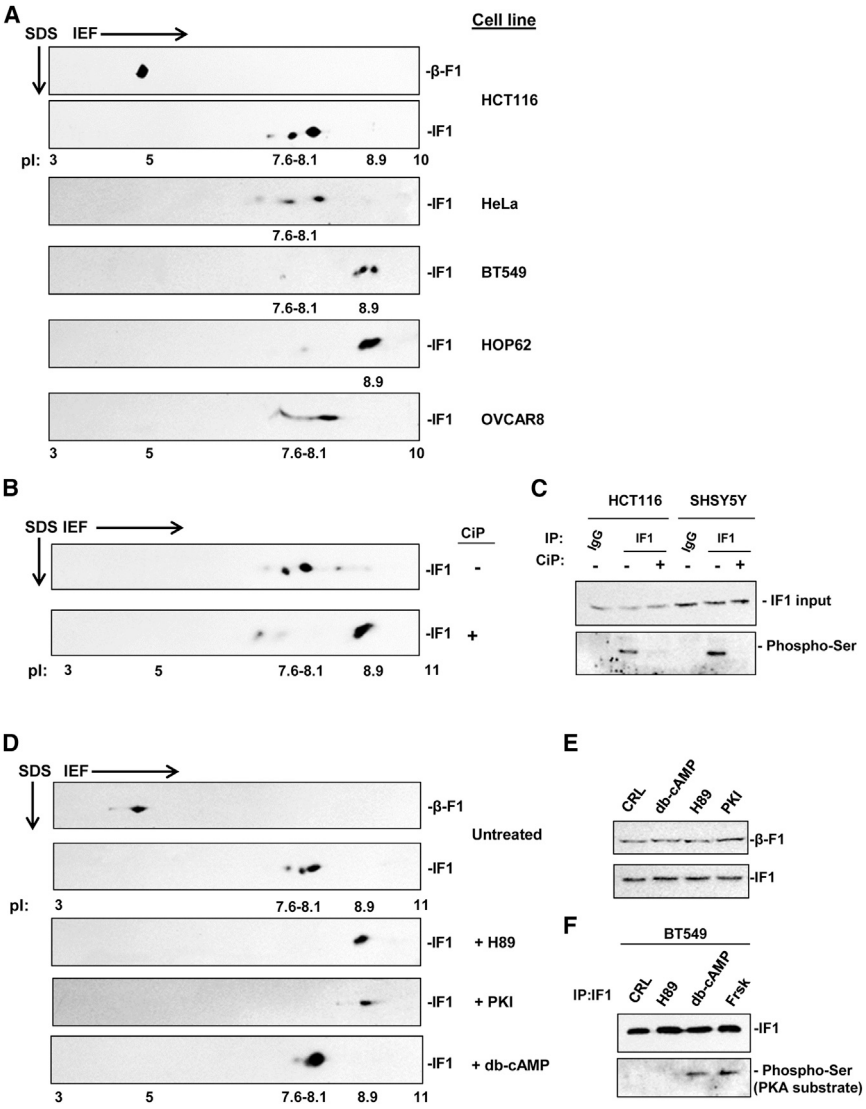

Figure 1. PKA Phosphorylates IF1

(A) Proteins from HCT116, HeLa, BT549, HOP62, and OVCAR8 cells were fractionated on 2D gels and blotted against anti-β-F1-ATPase (β-F1) and anti-IF1.

(B) Cellular proteins from HCT116 cells were fractionated and treated (+) or not (-) with CiP.

(C) Immunoprecipitated (IP) IF1 from HCT116 and SHSY5Y cellular extracts were treated (+) or not (-) with CiP and blotted with anti-phospho-Ser antibody. Non-specific immunoglobulin G (IgG) was included as control.

(D) HCT116 cells were treated with the PKA inhibitor H89 or PKI, or with db-cAMP, and the cellular extracts were fractionated on 2D gels. In (A), (B), and (D), the pI range of the strips and that of the focused proteins are indicated under the blots.

(E) HCT116 cells treated with db-cAMP, H89, or PKI revealed no changes in the steady-state content of IF1 when compared to untreated control cells (CRL).

(F) BT549 cells were left untreated (CRL) or treated with H89, db-cAMP, or Frsk, and the phosphorylated IF1 was revealed by incubation with the PKA phospho-serine residue antibody in the immunoprecipitated IF1.

fractionated on two-dimensional (2D) gels revealed the existence of protein isoforms of IF1 that differed in the isoelectric point (pI) depending on the cell line considered (Figure 1A). Focusing of β-F1-ATPase was used as a control (Figure 1A). In breast and lung cancer cells, the main isoform of IF1 has a pI of 8.9, close to the theoretical pI of the protein. In contrast, in colon, cervix, and ovarian cancer cells, IF1 appeared as two main isoforms, with pIs in the range of 7.6–8.1 (Figure 1A). The existence of more acidic isoforms differing in the pI of the protein suggested the covalent modification of IF1 by phosphorylation. This was confirmed in HCT116 cells by treatment of cell lysates with CiP (calf-intestinal alkaline phosphatase), which promoted the shift of IF1 to the basic region of the gel (pI = 8.9) (Figure 1B). Immunoprecipitation experiments with anti-IF1 of cellular extracts preincubated or not with CiP and blotting with antibodies against anti-phospho-Ser confirmed the presence of phosphorylated serines in IF1 in HCT116 and SHSY5Y cells (Figure 1C).

IF1 Is Phosphorylated by PKA

Cyclic AMP (cAMP)-dependent protein kinase A (PKA) is a predicted kinase that might be involved in the phosphorylation of IF1 (NetPhos 2.0; PhosphoMotif Finder). PKA is known to regulate mitochondrial respiration through phosphorylation of cytochrome c oxidase (Acin-Perez et al., 2009, 2011) and/or complex I (Papa et al., 2008). To this end, HCT116 cells were treated with different activators or inhibitors of PKA, and the IF1 isoforms were analyzed on 2D gels (Figure 1D). Treatment of the cells with two different inhibitors of the activity of PKA—the pseudosubstrate inhibitory peptide PKI (protein kinase inhibitor) or the competitive inhibitor H89 (Figure 1D)—revealed IF1 in its dephosphorylated state (pI = 8.9) (Figure 1D). In contrast, when cells were treated with the membrane-permeable PKA activator dibutyryl cAMP (db-cAMP), all IF1 was phosphorylated (pI = 7.6–8.1) (Figure 1D) in the absence of relevant changes on the content of IF1 (Figure 1E).

Western blots of immunoprecipitated IF1 from BT549 cells, which showed most of IF1 in its dephosphorylated state (pI = 8.9) (Figure 1A), revealed no immunoreactivity toward the specific PKA anti-phospho-Ser antibody when the cells were left untreated or treated with the PKA inhibitor H89 (Figure 1F). In contrast, phosphorylated IF1 was immunoprecipitated from BT549 cells treated with db-cAMP or with the adenylyl cyclase activator forskolin (Frsk) (Figure 1F), further supporting the differential regulation of IF1 phosphorylation by PKA in different

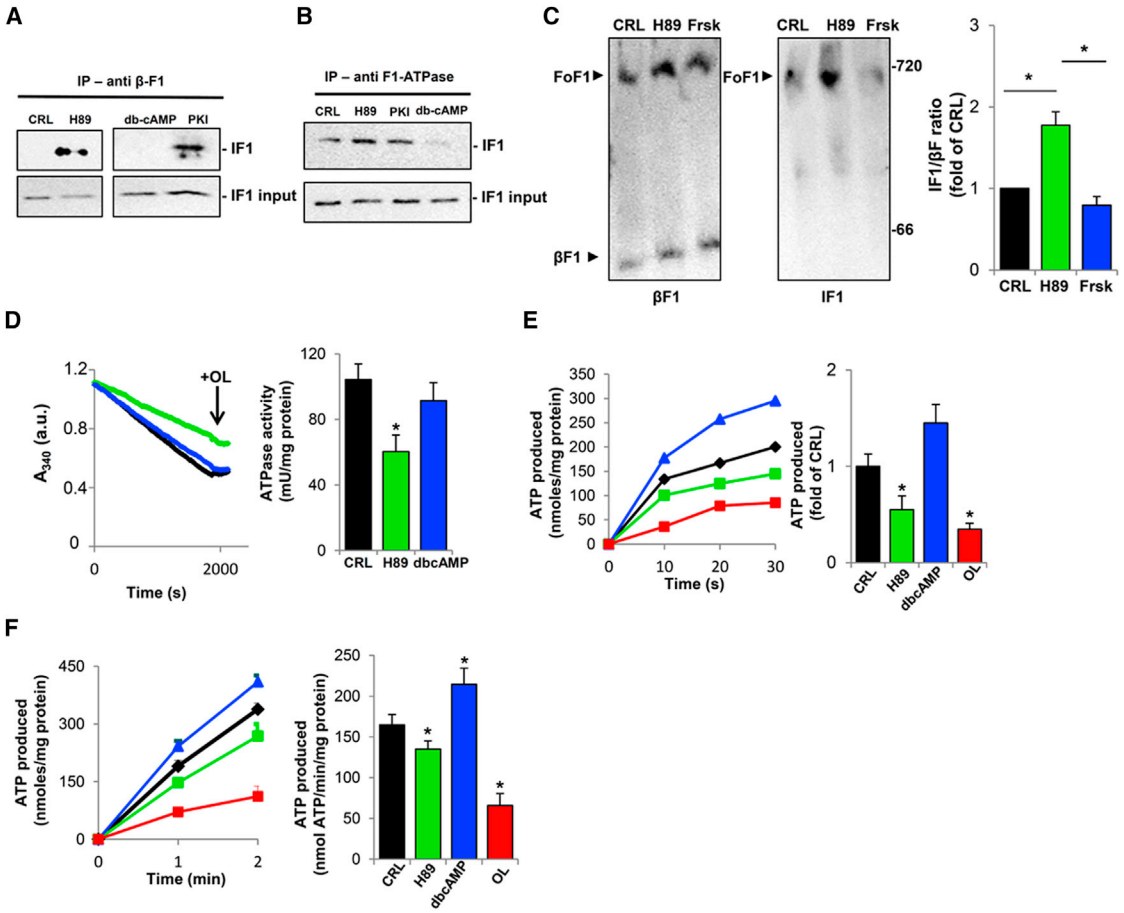

Figure 2. Dephospho-IF1 Binds and Inhibits the Hydrolase and Synthase Activities of the H^+-ATP Synthase

(A) HCT116 cells treated with H89, PKI, or db-cAMP or left untreated (CRL) were immunoprecipitated with anti-β-F1-ATPase, and the co-immunoprecipitated IF1 was identified by western blotting.

(B) Same as in (A), but immunoprecipitation was carried out with anti-F1-ATPase antibody.

(C) BN immunoblot analysis from HCT116 cells left untreated (CRL) or treated with H89 or Frsk. The migration of Complex V (FoF1) and IF1 is identified by reaction against anti-β-F1-ATPase and anti-IF1 antibodies, respectively. Migration of molecular mass markers is indicated. The histograms show the IF1/βF1 ratio of three different experiments.

(D) Hydrolase activity of the H^+-ATP synthase in isolated mitochondria from untreated HCT116 (CRL, black) and from H89 (green)-, and db-cAMP (blue)-treated cells. Where indicated, 30 μM OL was added. A_{340}, absorbance at 340 nm.

(E) Rates of ATP production in isolated mitochondria from HCT116 cells.

(F) Rates of ATP production in digitonin-permeabilized HCT116 cells.

Bars indicate the mean ± SEM of four to five different samples. *$p < 0.05$ when compared to CRL by Student's t test.

cancer cells (Figure 1A). In vitro PKA phosphorylation assays of IF1 resulted unsuccessfully (Figures S1A and S1B), suggesting that phosphorylation of IF1 might require scaffolding proteins.

Dephosphorylation of IF1 Promotes Its Binding to the F1-ATPase Complex

First, we studied the effect of IF1 phosphorylation on its capacity to bind the F1-ATPase complex (Figure 2A). Co-immunoprecipitation experiments of IF1 with a polyclonal antibody against the β-F1-ATPase subunit were carried out in HCT116 cells that were left untreated or treated with inhibitors (H89 and PKI) or the activator (db-cAMP) of IF1 phosphorylation (Figure 2A). Basal untreated HCT116 cells or cells treated with db-cAMP showed no co-immunoprecipitation of IF1 with the β subunit of the H^+-ATP synthase (Figure 2A). In contrast, cells treated with H89 and PKI—and, hence, with most of IF1 in its dephosphorylated state—showed high levels of IF1 co-immunoprecipitated with β-F1-ATPase (Figure 2A). Similar experiments were carried out using another antibody against the F1-ATPase complex, confirming that the dephosphorylation status of IF1 is required for its interaction and binding to the H^+-ATP synthase (Figure 2B). Interestingly, we noted that, in some experiments, a low amount of IF1 could be immunoprecipitated from control HCT116 cells (compare CRL in Figures 2A and 2B), suggesting a potential regulation of the phosphorylation of IF1 upon cellular conditions (discussed later). Consistent with these findings, Blue Native (BN) gels of mitochondrial membrane proteins from HCT116 cells revealed that the amount of IF1 bound to the ATP synthase

was increased in cells treated with H89 when compared to control or Frsk-treated cells (Figure 2C).

Dephosphorylated IF1 Inhibits Both the Synthase and Hydrolase Activities of the H^+-ATP Synthase

HCT116 cells were incubated with H89 or db-cAMP or were left untreated prior to mitochondrial extraction to study the effect of IF1 phosphorylation on the hydrolase and synthase activities of the enzyme (Figures 2D and 2E). Mitochondria from H89-treated cells containing dephosphorylated IF1 showed a diminished ATP hydrolase activity when compared to controls (Figure 2D), suggesting that phosphorylation of IF1 prevents its inhibitory action on the hydrolase. db-cAMP-treated cells displayed almost the same ATP hydrolase activity as that of control untreated cells (Figure 2D). Likewise, determination of the ATP synthetic activity of the enzyme in isolated mitochondria revealed that the production of ATP when IF1 is in its dephosphorylated state (H89 in Figure 2E) is diminished when compared to control mitochondria and similar to that of mitochondria incubated with oligomycin (OL) (Figure 2E). A slightly enhanced ATP synthetic capacity was observed in cells treated with db-cAMP (Figure 2E). Moreover, the ATP synthetic activity of the enzyme assessed in digitonin-permeabilized HCT116 cells treated with H89 showed a significant inhibition when compared to control cells (Figure 2F). In contrast, cells treated with db-cAMP significantly increased the rate of ATP synthesis in this situation (Figure 2F). Overall, the results support that dephosphorylated IF1 binds and inhibits the H^+-ATP synthase both in hydrolytic and synthetic modes, whereas phosphorylated IF1 is unable to bind and, hence, to interfere with the normal and reverse activities of the H^+-ATP synthase.

Phosphorylation of Serine 39 Is the Switch-Off Button

To identify the potential serine residues involved in regulating the activity of IF1 on the H^+-ATP synthase we created the phospho-mutant (S27A, S39A, and S63A) and phospho-mimetic (S27E, S39E, and S63E) point mutants of the serine residues present in the mature IF1 protein (Figure S1C; Table S1). To comply with the nomenclature of previous phosphoproteomic studies, the mutants are defined by residue number in the full-length IF1 sequence unless explicitly mentioning the residue in the mature protein. Transfection of HCT116 cells with a plasmid encoding the wild-type version of IF1 triggered a large overexpression of the dephosphorylated protein (Figure 3A) and the partial inhibition of the synthesis of ATP when compared to control cells transfected with the empty vector (EV) (Figure 3B). It should be noted that the cellular stress triggered by transfection already promoted dephosphorylation of IF1 (EV; Figure 3A). Analysis of the effect of the expression of the phospho-mutant and phospho-mimetic constructs on ATP synthesis assessed in permeabilized cells revealed that only S39A had a significant negative effect on the activity when compared to the wild-type IF1 or to the corresponding phospho-mimetic S39E, which presented a similar ATP output to EV-transfected cells (Figure 3B). Consistent with a role for the phosphorylation of S39 in regulating IF1 activity, we observed that Frsk-treated cells overexpressing S39A did not relieve the inhibition on the ATP synthase activity (Figure 3C), as it occurs in cells expressing wild-type IF1 (Figure 3C). As expected, cells expressing S39E showed higher ATP synthase activities than cells expressing wild-type IF1, further revealing no major differences when incubated with H89 or Frsk (Figure 3C).

As shown earlier (Figures 2A and 2B), the inhibition of the ATP synthase correlated with the binding of IF1 to F1-ATPase as revealed by co-immunoprecipitation of the inhibitory S39A mutant with β-F1-ATPase (Figure 3D) and the negligible pull-down of the non-inhibitory S39E in the same situation (Figure 3D). Co-immunoprecipitation of S39A and β-F1-ATPase also occurred when cells were treated with Frsk (Figure 3E). Moreover, BN gels also showed that interaction with the ATP synthase only occurs when the S39A mutant is being expressed (Figure 3F). Overall, the results support that phosphorylation of S39 is a main player in preventing the binding and inhibition of IF1 on the ATP synthase.

Dephosphorylated IF1 Inhibits OXPHOS and Enhances Aerobic Glycolysis

Consistent with previous findings showing that PKA-mediated phosphorylation affects the activity of mitochondrial respiratory complexes, we observed that cells treated with H89 and PKI had reduced respiratory rates (Figure 4A). OL-sensitive respiration (OSR) is a measure of the activity of the H^+-ATP synthase. To verify that the effect of PKA on OSR was mainly due to IF1 and not to the effect of PKA on other proteins of the OXPHOS (oxidative phosphorylation) system, we performed the same experiments but in silenced IF1 cells (Figure 4B). The results revealed that silencing of IF1 reverted the effect of H89 on OSR (Figure 4B), supporting that dephosphorylated IF1 is inhibiting the synthetic activity of the H^+-ATP-synthase in cells in culture.

The inhibition of OXPHOS by IF1 is balanced by a burst in aerobic glycolysis (Sánchez-Cenizo et al., 2010). Hence, we determined the glycolytic flux by measuring the initial rate of lactate production (Figure 4C). Aerobic glycolysis was upregulated in cells treated with PKA inhibitors and was not affected when cells were incubated with db-cAMP (Figure 4C). Silencing of IF1 prior treatment with both PKA inhibitors also resulted in blunting the upregulation of aerobic glycolysis (Figure 4D). Overall, we show that the phosphorylation of IF1 determines its biological activity and, therefore, that its regulation mediates cellular reprogramming of energy metabolism.

IF1 and the Flux of Energy Provision Pathways

We compared the phosphorylation of IF1 of HCT116 cells growing in the presence of OL versus that of cells growing in the presence of 2-deoxyglucose (2DG) (Figure 5A), which are known to regulate the flux of energy metabolism through glycolysis and OXPHOS, respectively (Figure 5A) (Sánchez-Aragó et al., 2010). Despite the presence of OL, we observed that a fraction (~30%) of IF1 becomes dephosphorylated when HCT116 cells are incubated with OL (Figure 5A). Incubation of the cells with 2DG, which upregulates OXPHOS, does not significantly affect the phosphorylation of IF1 (Figure 5A). Similar experiments in BT549 cells that have most of IF1 dephosphorylated in basal state (Figure 1A) revealed the opposite situation showing a shift of a fraction of IF1 (~30%) toward a more

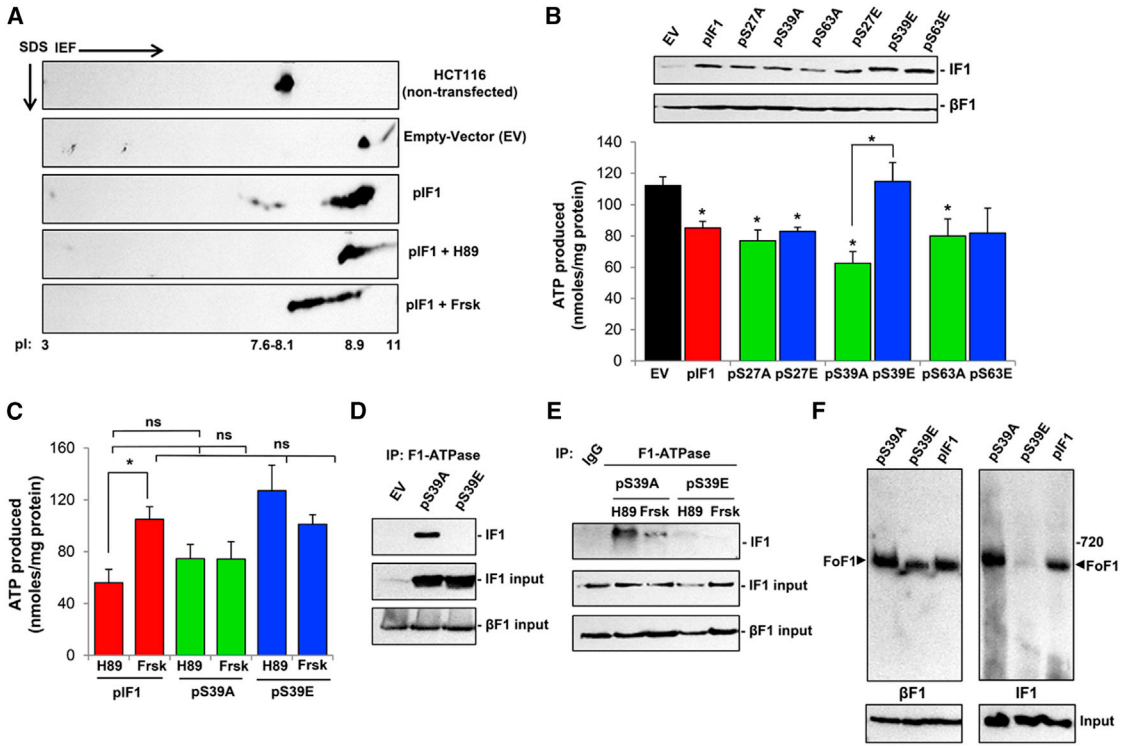

Figure 3. Phosphorylation of S39 Regulates the Activity of IF1

(A) HCT116 cells non-transfected or transfected with EV or with pIF1 were treated with H89 or Frsk and fractionated on 2D gels.

(B) ATP synthase activity in permeabilized HCT116 cells expressing wild-type IF1 (pIF1, red), IF1 phospho-mutant (pS27A, pS39A, and pS63A; green), or IF1 phospho-mimetic (pS27E, pS39E, and pS63E; blue) constructs.

(C) Same as in (B), but treated with H89 or Frsk.

(D and E) HCT16 cells transfected with EV, pS39A, or pS39E non-treated (D) or treated with H89 or Frsk (E) were immunoprecipitated (IP) with anti-F1-ATPase, and the co-immunoprecipitated IF1 was identified.

(F) BN immunoblot of mitochondrial membrane proteins from HCT116 cells transfected with pIF1, pS39A, or pS39E. The migration of Complex V (FoF1) and IF1 is shown, along with input levels of both proteins.

In (B) and (C), error bars indicate the mean ± SEM of four to five different samples. *$p < 0.05$, when compared to CRL by Student's t test. ns, non-significant.

phosphorylated state when the cells are incubated in the presence of 2DG (Figure 5B). Consistently, changes in the phosphorylation status of IF1 in BT549 cells also correlated with an increase in the activity of OXPHOS, as revealed by OSR and the reduction of aerobic glycolysis (Figure 5B).

IF1 and Progression through the Cell Cycle

Cell cycle progression is known to affect the relative activity of the main energy provision pathways of the cell (Chen et al., 2007). Whereas the G1 phase is largely dependent on OXPHOS, the reductive G2/M phase depends on aerobic glycolysis and is largely independent of oxygen consumption. Hence, we compared the phosphorylation of IF1 of HCT116 cells arrested in G1 by incubation with the DNA-polymerase inhibitor aphidicolin (Figure 5C) versus that of cells arrested in G2/M by incubation with nocodazole, a disruptor of the mitotic spindle (Figure 5C). The results showed that most of IF1 was phosphorylated in G1 cells, whereas dephosphorylated IF1 was present in cells arrested in G2/M (Figure 5D). Consistently, the changes in IF1 phosphorylation nicely correlated with the relative activity of OXPHOS and aerobic glycolysis in the different phases of the cell cycle, with dephosphorylated IF1 being concurrent with repressed OXPHOS and an enhanced aerobic glycolysis of the cells (Figure 5D).

IF1 and Cellular Hypoxia

Cellular hypoxia, induced either by oxygen deprivation or chemically by incubation of the cells with $CoCl_2$, promotes the arrest of OXPHOS (OSR in Figure 6A) and triggers aerobic glycolysis (Figure 6A). Consistently, we observed the shift of IF1 toward the dephosphorylated state in hypoxic cells (Figure 6B). The concurrent inhibition of both the ATP hydrolase (Figure 6C) and ATP synthetic (Figure 6D) activities of the H^+-ATP synthase by hypoxia was confirmed in isolated mitochondria (Figure 6C) and in permeabilized HCT116 cells (Figure 6D), respectively. Interestingly, silencing of IF1 in cells treated with $CoCl_2$ blunted the inhibition of the hydrolase and synthetic activities of the H^+-ATP synthase (Figure S2). Moreover, incubation of the cells with $CoCl_2$ in the presence of Frsk enhanced both the ATPase (Figure 6C) and synthase (Figure 6D) activities of the enzyme. Consistently, the IF1-mediated inhibition of the ATP synthase in $CoCl_2$-treated cells also correlated with an enhanced binding of IF1 onto the

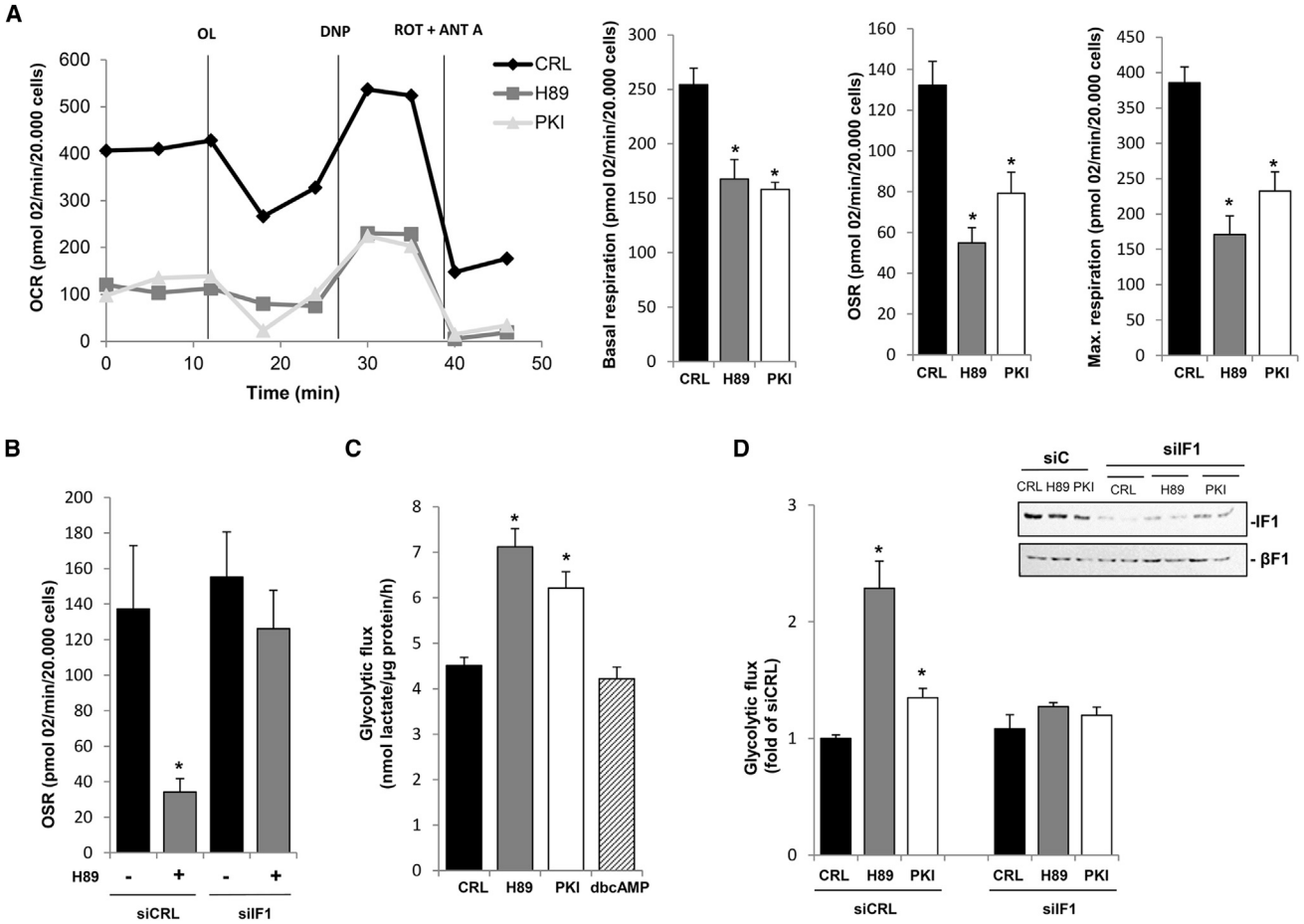

Figure 4. Dephosphorylation of IF1 Reprograms Energy Metabolism

HCT116 cells were treated with H89 (gray bar), PKI (open bar), db-cAMP (hatched bar), or left untreated (CRL; closed bar).

(A) The respiratory profile, the basal rate, OSR, and maximum respiratory rates are shown. OCR, oxygen consumption rate; DNP, 2,4-dinitrophenol; ROT + ANT A, rotenone + antimycin A.

(B) Cells transfected with control (siCRL) or siIF1 siRNA (siIF1) were treated (+) or not (-) with H89.

(C and D) In (C), the initial rates of lactate production were determined after cellular treatments. In (D), cells were transfected with control (siCRL or siC) or siIF1 siRNA (siIF1) and after treated as indicated. The silencing of IF1 was verified by western blot.

Error bars are the mean ± SEM of three experiments. *$p < 0.05$ when compared to CRL by Student's t test.

enzyme, as revealed by BN gels (Figure 6E), further supporting the role of IF1 in reprogramming energy metabolism.

IF1 Is Dephosphorylated in Prevalent Human Carcinomas

We have recently stressed the contribution of IF1 to the glycolytic phenotype in some human carcinomas (Formentini et al., 2012; Sánchez-Aragó et al., 2013b; Sánchez-Cenizo et al., 2010). To assess the phosphorylation status of IF1 in tumor samples from human patients, we used phosphate-affinity (Phos-tag) PAGE and western blotting (Kinoshita et al., 2009). Consistently, incubation of the samples with the phosphatase (CiP in Figure 6F) abrogates the differences in electrophoretic migration between phospho-IF1 (p-IF1) and IF1. Phos-tag immunoblot analysis indicated that most colorectal carcinomas (Figure 6F), breast adenocarcinomas (Figure 6G), and lung squamous cell carcinomas (Figure 6H) and adenocarcinomas (Figure 6I) have IF1 in its dephosphorylated state, strongly supporting a role for IF1 as inhibitor of the H^+-ATP synthase and, hence, of OXPHOS in human cancers.

Activation of PKA Triggers the Phosphorylation and Inactivation of IF1 in Heart In Vivo

Stimulation of cardiac β-adrenoceptors is crucial to increase heart function under stress (Steinberg and Brunton, 2001). Their coupling to stimulatory G proteins (Gs) triggers the activation of adenylyl cyclase, which generates the cAMP involved in downstream signaling through the activation of PKA. To test in vivo the relevance of IF1 phosphorylation, we treated mice with clenbuterol, a β-adrenergic agonist, and assayed the phosphorylation status of IF1 in parallel with the ATP synthase and hydrolase activities of the enzyme in isolated heart mitochondria. Other

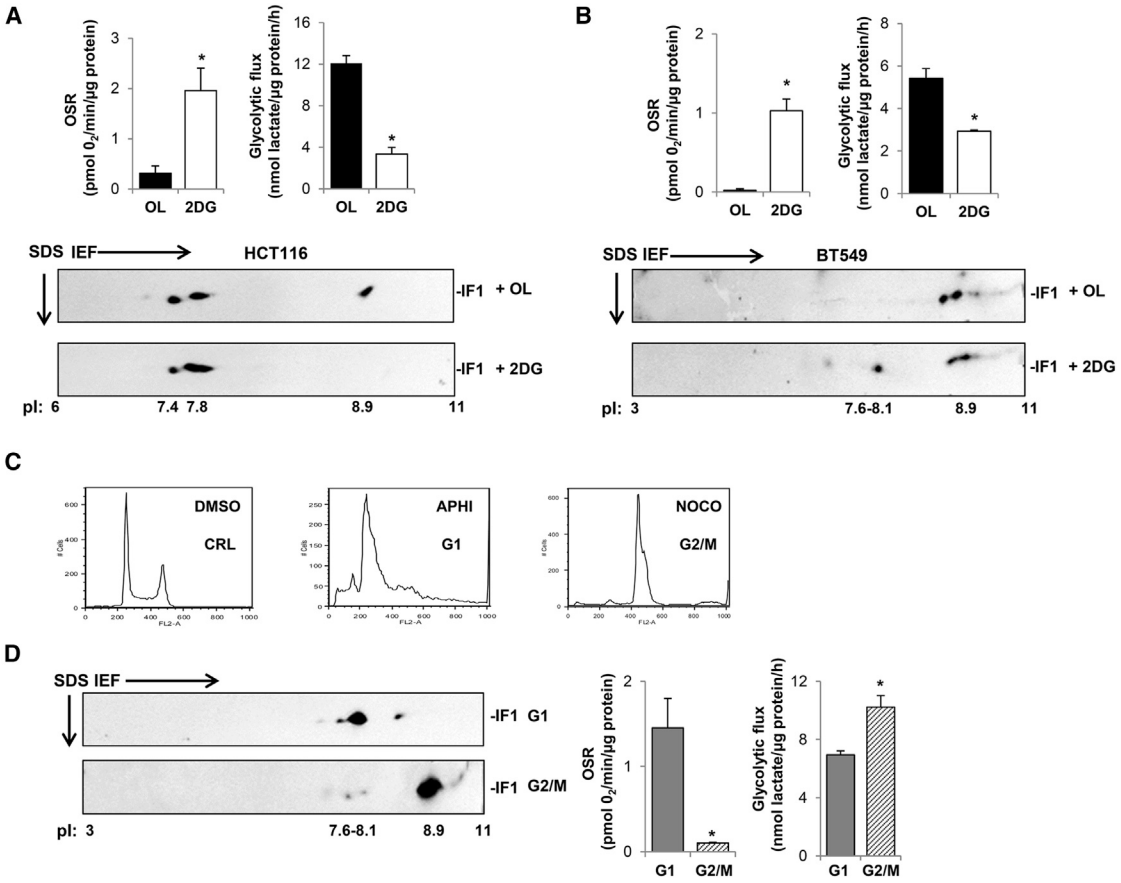

Figure 5. Energy Demand Determines IF1 Phosphorylation

(A–D) HCT116 cells in (A), (C), and (D) and BT549 cells in (B) were treated with OL (closed bars), 2DG (open bars), aphidicolin (APHI; gray bars), or nocodazole (NOCO; hatched bars), and the OSR, initial rates of lactate production, and the phosphorylation of IF1 were determined. The pI range of the strips and of the focused proteins is indicated under the blots. In (C), the cell cycle of treated cells was analyzed. The histograms in (A), (B) and (D) indicate the mean ± SEM of 8–10 different samples. *$p < 0.05$ when compared to control by Student's t test.

mice were treated with propranolol, a β-adrenergic antagonist. Interestingly, ~50% of IF1 in mouse heart is found in its phosphorylated state (mouse 2 in Figure 7A). The administration of clenbuterol promotes a sharp increase in the phosphorylation of IF1 (mice 1, 4, and 5 in Figure 7A) that is abrogated by incubation of heart extracts with CiP (mice 1, 4, and 5 in Figure 7A). Consistently, in this situation, we observed a sharp increase in the concentration of cAMP in isolated heart mitochondria (Figure 7B). In contrast, the administration of propanolol shifted the phosphorylation status of IF1 toward its dephosphorylated state (mouse 3 in Figure 7A) and had no effect on intramitochondrial cAMP (Figure 7B). Remarkably, a short 10-min incubation of isolated mitochondria in the presence of the membrane-permeable db-cAMP triggered the rapid and complete phosphorylation of IF1 (Figure 7C), supporting the participation of mitochondrial PKA in the regulation of IF1 phosphorylation. Overall, these findings support the hypothesis that, under β-adrenergic activation, when the energy demand is enhanced, most of the IF1 reserve of the cell becomes inactivated to prevent its binding to the H^+-ATP synthase in order to favor a higher output of ATP. Consistent with this suggestion, we observed that both the ATP hydrolytic (Figure 7D) and synthetic (Figure 7E) activities of the H^+-ATP synthase assayed in isolated heart mitochondria of clenbuterol-treated mice were significantly higher than that in mitochondria of control, saline-treated mice. In agreement with the shift toward dephosphorylated IF1 upon propranolol administration (Figure 7A), we observed that both activities of the H^+-ATP synthase were significantly reduced when compared to those of saline-treated mice (Figures 7D and 7E).

DISCUSSION

A long-standing principle is that IF1, the intrinsically disordered inhibitor of the H^+-ATP synthase (Bason et al., 2014; Gordon-Smith et al., 2001), is a unidirectional inhibitor of ATP hydrolysis, having no direct effect on ATP synthesis when in the presence of a proton motive force (Walker, 2013). However, previous data from our laboratory obtained in cells (Formentini et al., 2012; Sánchez-Aragó et al., 2013b, 2013c), and in a mouse model overexpressing an active IF1 in neurons (Formentini et al., 2014), support that in vivo IF1 also inhibits the synthase activity of the H^+-ATP synthase. Herein, we demonstrate that, when

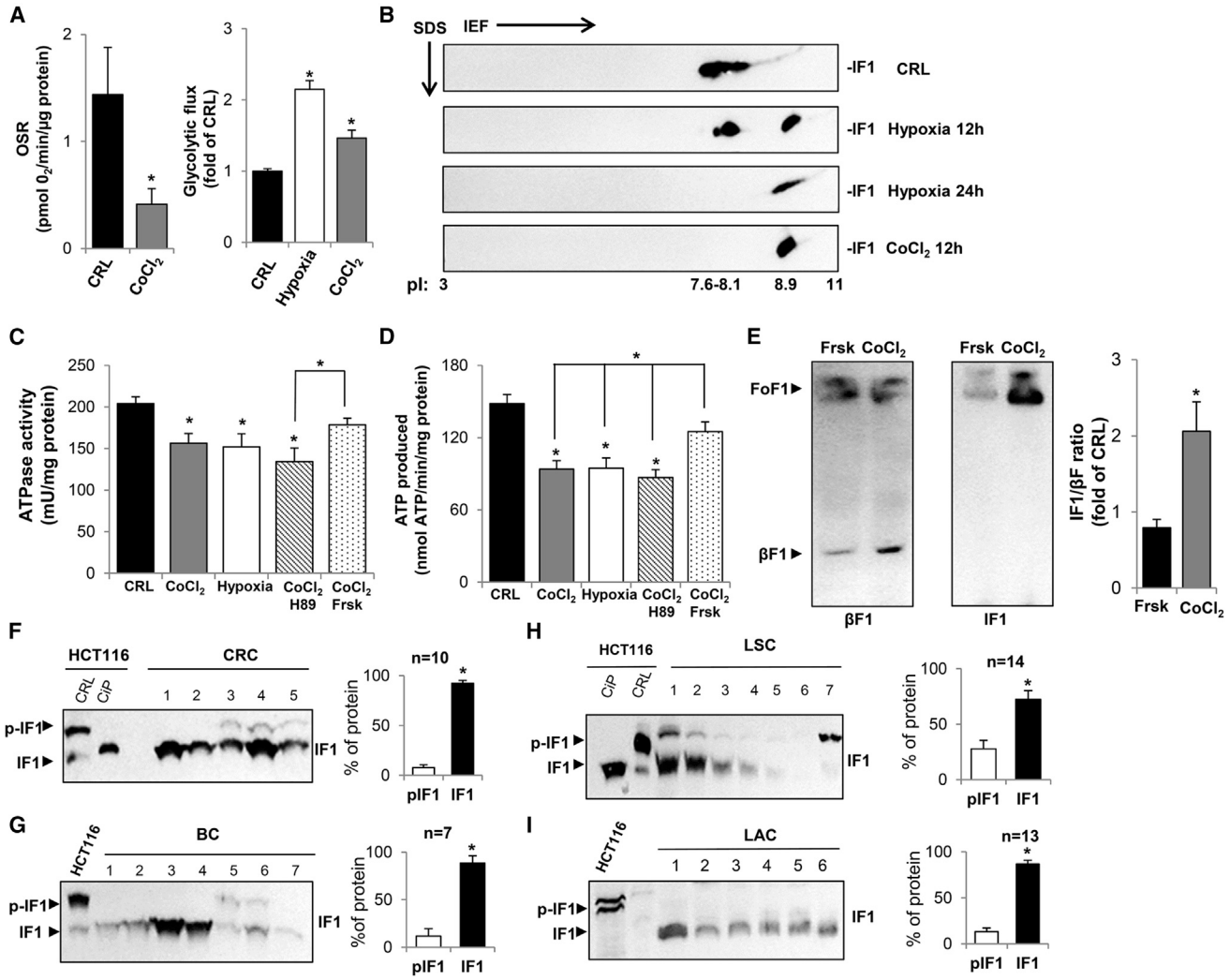

Figure 6. Hypoxia and Cancer Trigger the Dephosphorylation of IF1

(A–D) HCT116 cells were left untreated (CRL, closed bar), treated with $CoCl_2$ (gray bar), or subjected to oxygen deprivation (open bar). $CoCl_2$ treatment was also added along with H89 (hatched bar) or Frsk (dotted bar). The OSR and initial rates of lactate production (A) and the analysis of IF1 phosphorylation (B) were determined. In (C), hydrolase activity of the H^+-ATP synthase was determined in isolated mitochondria. In (D), rates of ATP production in permeabilized HCT116 cells are given. The histograms in (A), (C), and (D) indicate the mean ± SEM of three experiments.

(E) BN immunoblot of mitochondrial membranes from HCT116 cells treated with Frsk or $CoCl_2$. The co-migration of the ATP synthase (FoF1) with IF1 is shown by blotting with anti-β-F1-ATPase and anti-IF1 antibodies, respectively. The histogram shows the IF1/βF1 ratio of three different experiments.

(F–I) Phos-tag SDS-PAGE analysis of the phosphorylation of IF1 in human extracts of colorectal carcinomas (CRC) in (F), breast carcinomas (BC) in (G), lung squamous cell carcinomas (LSC) in (H), and lung adenocarcinomas (LAC) in (I). Histograms represent the percentage of phospho-IF1 (p-IF1, open bars) and dephosphorylated IF1 (IF1, closed bars) in the samples.

Bars indicate the mean ± SEM. The number of studied patients is indicated. *$p < 0.05$ when compared to CRL by Student's t test.

IF1 is dephosphorylated, it inhibits both the synthase and hydrolase activities of the enzyme, as assessed in permeabilized cells and in isolated mitochondria from cells and mouse hearts. We show that IF1 is subjected to reversible post-translational modification by phosphorylation, most probably through the activation of mitochondrial PKA. Mechanistically, we demonstrate that phosphorylation of IF1 in S39 impedes its interaction with the H^+-ATP synthase, hampering in this way its potential as an inhibitor of the enzyme. Moreover, we unveil the relevance that the phosphorylation of IF1 has for understanding the physiological role that this protein plays in the mitochondrial adaptations that require metabolic rewiring, such as in the response to an increased demand for ATP provision by OXPHOS in vivo or in the activation of aerobic glycolysis during progression through the cell cycle, in hypoxia, and in human carcinomas. Overall, the phosphorylation of IF1 acts as the molecular switch that regulates the inhibitory activity of IF1 on the synthase, hence revealing a mechanism to coordinate metabolic activity in the cytoplasm and in mitochondria in response to changes in cellular signaling aimed at satisfying the fluctuating energy demand.

Previous reports have described the phosphorylation of S39 and S63 of human IF1, which, in the mature protein, correspond to S14 and S38, respectively (see Figure S1C). Herein, we show that phosphorylation of S39/S14 determines the biological activity of the protein by preventing its interaction with the H^+-ATP synthase. Phosphorylation of IF1 is not restricted to a small fraction of the protein but rather can affect the whole pool of IF1, as revealed in different metabolic situations. IF1 has been described as an intrinsically disordered protein (Gordon-Smith et al., 2001), as this conformation of the inhibitor is essential for its initial interaction with the F1-ATPase domain of the H^+-ATP synthase (Bason et al., 2014) (Figure 7F). Intrinsically disordered proteins are important components of cellular signaling, because conformational disorder-to-order transitions mediate biological function (Wright and Dyson, 2015) and protein phosphorylation is known to regulate these transitions (Bah et al., 2015). Hence, we suggest that phosphorylation of S39/S14 might promote the folding of the intrinsically disordered IF1 and that this conformational transition would impede its capacity to grasp and enter its binding site on F1-ATPase (Figure 7F) (Bason et al., 2014). We cannot exclude that steric hindrance and/or electrostatic repulsions of the phosphorylated S39/S14 could also contribute in interfering the binding of IF1. Interestingly, the highly conserved S39/S14 is placed at the initiation of the single α-helical turn that interacts with the γ-subunit (Figure 7G) (Bason et al., 2014).

The activity of PKA is involved in the phosphorylation of IF1, triggering the activation of the synthase and hydrolase activities of the H^+-ATP synthase and thus supporting that IF1, when bound to the enzyme, inhibits both activities (Figure 7H). The activation of OXPHOS mediated by cAMP/PKA signaling is in agreement with previous reports by others (Acin-Perez et al., 2009; Di Benedetto et al., 2013; Livigni et al., 2006; Papa et al., 2008). However, it should be noted that the physiological relevance, mitochondrial substrates, and the site of PKA action are still a matter of debate (Di Benedetto et al., 2014; Valsecchi et al., 2013), despite PKA being described in the mitochondria of a wide range of mammalian species (Pagliarini and Dixon, 2006). Moreover, PKA has been recently described to be associated with high-molecular-weight complexes of the inner mitochondrial membrane (Acín-Pérez et al., 2014). In this line, it is well established that the activation of the β-adrenergic/adenylyl cyclase/cAMP/PKA signaling pathway in cardiac muscle results in the phosphorylation and activation of protein targets involved in the provision of metabolic precursors for oxidative purposes (Christian et al., 1969), concurrently with a raise of cytoplasmic Ca^{2+} (Kamp and Hell, 2000), which is a key element for the activation of OXPHOS (Glancy and Balaban, 2012). Intracellular Ca^{2+} triggers the contraction of muscle fibers and is subsequently sequestered by mitochondria (Rizzuto et al., 2012), where it could activate the soluble adenylyl cyclase that has been shown to be regulated by bicarbonate (Acin-Perez et al., 2009) and Ca^{2+} (Di Benedetto et al., 2013), building up intramitochondrial cAMP, as we have observed in the heart mitochondria of clenbuterol-treated mice. Since cAMP is not permeable across mitochondrial membranes (Di Benedetto et al., 2013) and we have observed the rapid phosphorylation of IF1 in isolated mitochondria in response to the permeable db-cAMP, we suggest that phosphorylation of IF1, similarly to COXIV-1 (Acin-Perez et al., 2011), could be exerted inside mitochondria by PKA or a PKA-like enzyme (Figure 7H) (Acin-Perez et al., 2009; Di Benedetto et al., 2014; Valsecchi et al., 2013).

In our hands, PKA is unable to phosphorylate IF1 in in vitro assays, suggesting the requirement of additional proteins for IF1 phosphorylation. Three major A-kinase anchor proteins (AKAPs) targeting PKA to mitochondria have been described: AKAP-121 (Huang et al., 1997) and WAVE-1 (Danial et al., 2003), which tether PKA to the outer mitochondrial membrane, and sphingosine kinase interacting protein (SKIP), which is mainly enriched in the inner mitochondrial membrane (Means et al., 2011). Targeting of AKAP-121 to mitochondria produces a burst in OXPHOS (Livigni et al., 2006). Hence, we cannot rule out that IF1 might be phosphorylated by mitochondrial PKA assisted by as-yet-unidentified anchoring proteins. Moreover, it is reasonable to suggest that dephosphorylation of IF1—and, hence, the activation of its inhibitory function—might be exerted by a mitochondrial phosphatase (Figure 7H). However, since IF1 is a mitochondrial protein with a very short half-life of ~120 min (Sánchez-Aragó et al., 2013b), it is also possible that its high rate of turnover could reestablish its potential inhibitory activity on the H^+-ATP synthase.

The primary biological role suggested for IF1 is to act as the mitochondrial protein that, in situations that compromise the proton motive force (hypoxia), prevents ATP hydrolysis and the waste of biological energy (Campanella et al., 2008; Gledhill et al., 2007; Walker, 2013) (Figure 7H). In line with this idea, the disaggregation and activation of IF1 appear to be controlled by the ionic state of a histidine residue (H49) that is thought to provide a pH-sensitive switch between inactive and active states of the protein at relatively low values of intramitochondrial pH (Cabezon et al., 2000). The mechanisms that we are now describing in no way compromises our understanding of the regulation of IF1 function by pH but rather amplifies it because only dephosphorylated IF1 is able to bind the synthase and inhibit its hydrolase activity. Moreover, it illuminates the paradox that we have previously stressed regarding the high expression levels of IF1 found in tissues with high energy demand (brain, kidney, liver, and heart) (Sánchez-Aragó et al., 2013b; Sánchez-Cenizo et al., 2010). In fact, we demonstrate a mechanism for the silencing of the inhibitory activity of IF1 on the H^+-ATP synthase (Figure 7H) that might affect a fraction of the expressed protein in these tissues. Indeed, the presence of the bulk of IF1 in mouse heart in both its phospho- and dephosphorylated states offers the possibility of a reservoir for an enhanced tissue capacity of OXPHOS in response to a burst of metabolic demand, as we have shown after treatment of mice with clenbuterol and the subsequent enhanced production of ATP by mitochondria (Figure 7).

Provided that dephospho-IF1 binds and inhibits the ATP synthetic activity of the enzyme, the question is, what might be the role for a fraction of inhibitory IF1 in highly demanding tissues? One answer might be that this fraction of IF1 is being used for the fine adjustment of the mitochondrial output of ATP. Perhaps, although a speculation at the present stage is that the inhibition of a fraction of the available H^+-ATP synthase by IF1 might be involved in cellular tuning by "mitohormesis" (Yun and Finkel, 2014). Indeed, IF1-mediated inhibition of the H^+-ATP synthase

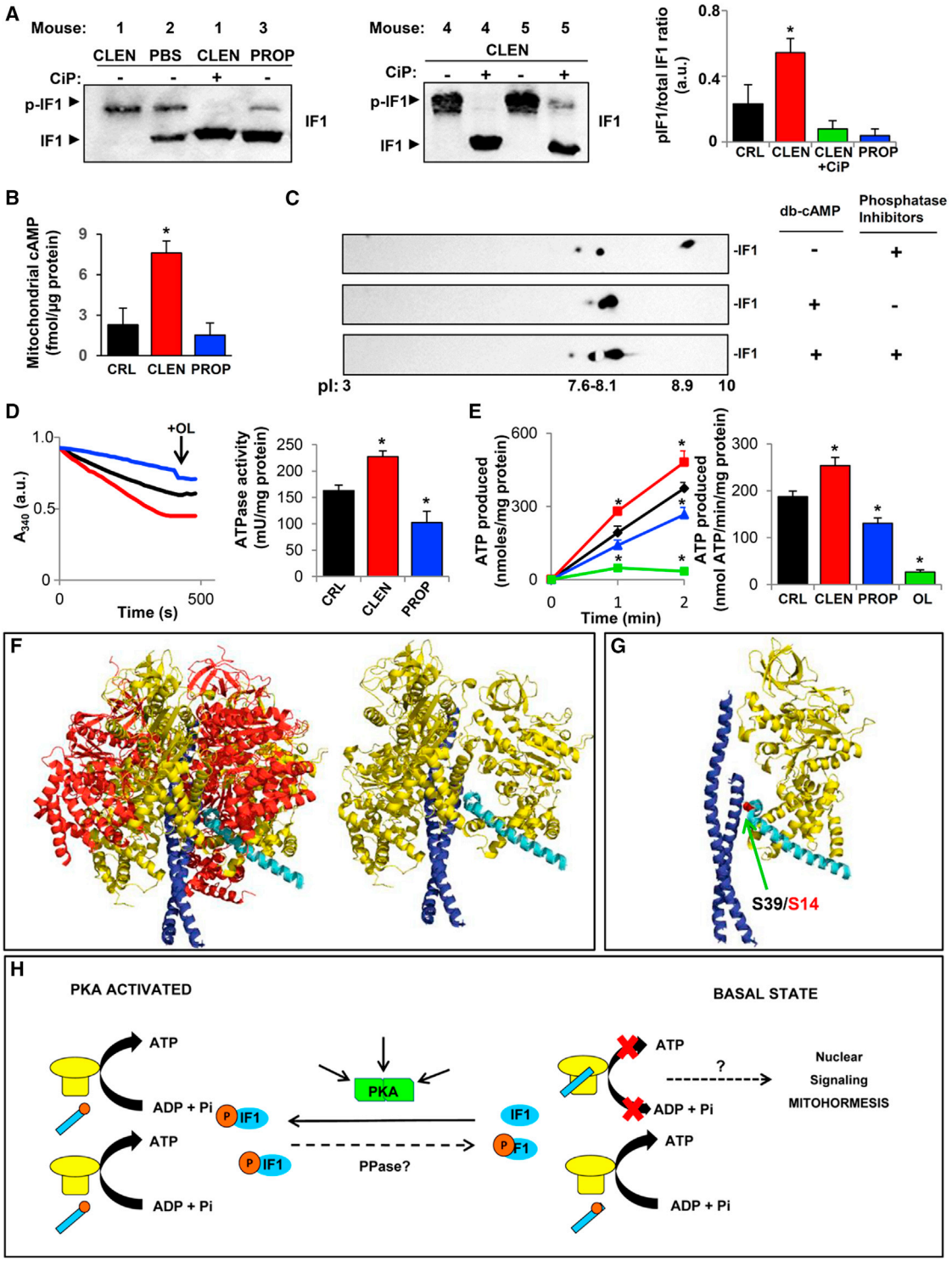

Figure 7. In Vivo Stimulation of PKA Promotes IF1 Phosphorylation and Its Inactivation

Mice were intraperitoneally injected with PBS (CRL; black traces and bars), 1 mg/kg clenbuterol (CLEN; red traces and bars), or 10 mg/kg propranolol (PROP; blue traces and bars).

(A) Phos-tag SDS-PAGE analysis of the phosphorylation of IF1 (p-IF1). CiP treatment of CLEN samples (green bars) were included as control. pIF1/total IF1 ratio is shown.

(B) cAMP in isolated heart mitochondria from mice treated as indicated.

(legend continued on next page)

has been shown to promote the production of superoxide radical (Formentini et al., 2012; Sánchez-Aragó et al., 2013b), a reactive oxygen species (ROS) signal of mild intensity that triggers nuclear reprogramming aimed at the activation of defense mechanisms to prevent cell death both in cancer cells (Formentini et al., 2012; Sánchez-Aragó et al., 2013b) and in neurons in vivo (Formentini et al., 2014) (Figure 7H). This speculation is further supported by the recent observations that the generation of mitochondrial ROS (Schaar et al., 2015) and the inhibition of the H^+-ATP synthase (Chin et al., 2014) positively affect lifespan extension, hence claiming a relevant role for IF1 and the H^+-ATP synthase in cell physiology.

EXPERIMENTAL PROCEDURES

Human Tumor Samples and Mouse Studies

Frozen tissue sections obtained from surgical specimens of untreated breast, lung, and colon cancer patients were processed. The project was approved by the Ethical Committee of the Universidad Autónoma de Madrid (CEI-24-571). For details, see the Supplemental Information. For mouse experiments, 12- to 20-week-old mice of the FVB genetic background were injected intraperitoneally with sterile PBS (GIBCO), 1 mg/kg clenbuterol (Sigma), or 10 mg/kg propanolol hydrochloride (Sigma) and sacrificed 12 hr after.

Cell Lines, Treatments, and siRNA Silencing

Human colorectal carcinoma HCT116 cells were grown in McCoy's 5A media. Details for other cell lines are provided in the Supplemental Information. Cells were treated with PKA agonists (100 μM db-cAMP or 40 μM forskolin) or inhibitors (10 μM competitive inhibitor H89 or 1 μM PKI fragment 6–22) for 12 hr before processing. Suppression of IF1 expression in HCT116 cells was performed using siPORT NeoFX Transfection Agent (Ambion) and a specific small interfering RNA (siRNA) (QIAGEN S100908075) at a final concentration of 20 nM. An inefficient siRNA sequence, Silencer Select Negative Control #1 (Ambion), was used as a control. For hypoxic stress, cells were treated either with 200 μM $CoCl_2$ for 12 hr or deprived of oxygen (1% O_2) for the indicated times in a Hypoxic Workstation H35 (Don Whitley Scientific). Dephosphorylation of proteins with CiP (New England Biolabs) was carried out by incubation of 50 μg of cellular extracts at 37°C for 1 hr with 20 U of CiP. Protein concentration was determined using the Bradford reagent using BSA as standard.

IF1 Mutants

Site-directed mutagenesis of IF1 to generate the phospho-mutants S27A, S39A, and S63A and phospho-mimetic S27E, S39E, and S63E constructs was performed with QuickChange Lightning (Agilent Technologies) using the primers indicated in Table S1 and the pCMV-SPORT6-IF1 plasmid (Sánchez-Cenizo et al., 2010).

2D and BN Gel Electrophoresis

Isoelectrofocusing (IEF) was performed with 13-cm Immobiline DryStrips of different pH gradients (pH 3–10 L [linear], pH 3–11 NL [nonlinear], or pH 6–11 L; GE Healthcare) using an Ettan IPGPhor3 IEF unit (GE Healthcare). For BN gels, isolated mitochondria were suspended in 50 mM Tris-HCl, pH 7.0, containing 1 M 6-aminohexanoic acid, at a final concentration of 10 mg/ml. The membranes were solubilized by the addition of 10% digitonin. 5% Serva Blue G dye in 1 M 6-aminohexanoic acid was added to the solubilized membranes. Additional details for 2D and BN gels are provided in Supplemental Information.

Immunoblot Analysis

Details of protein fractionation on SDS-PAGE and of the antibodies used in western blots are provided in the Supplemental Information.

Immunoprecipitation Assays

Cells were lysed on lysis buffer (50 mM Tris-HCl, pH 6.0, 150 mM NaCl, 0.5% Nonidet P40), complete EDTA-free protease inhibitor cocktail (Roche), and phosphatase inhibitor cocktail (Sigma). Protein from cell lysates (400 μg) was incubated with 12 μg of the indicated antibody bound to EZ View Red Protein G Affinity Gel at 4°C.

Aerobic Glycolysis and Oxygen Consumption Rates

The oxygen consumption rates (XF24 Extracellular Flux Analyzer, Seahorse Bioscience) and the initial rate of lactate production were determined as previously described (Sánchez-Cenizo et al., 2010).

Determination of the H^+-ATP Synthase Activities

Mitochondria isolated from HCT116 cells or from mouse hearts were used for the determination of the hydrolase activity of the enzyme (Formentini et al., 2014). The ATP synthetic activity was determined in isolated mitochondria and in digitonin-permeabilized cells (Vives-Bauza et al., 2007). Aliquots, taken at indicated time intervals, were precipitated with 6% $HClO_4$ and neutralized with 10% KOH, and the ATP content was determined using the ATP Bioluminiscence Assay Kit (Roche) to assess the linear rate of ATP synthesis (Mourier et al., 2014). Inhibition of the hydrolase and synthase activities of the H^+-ATP synthase was accomplished by the addition of 30 μM OL.

Determination of cAMP

cAMP levels were determined in 200 μg of isolated heart mitochondrial protein using the cAMP Direct Immunoassay Kit (Abcam).

Phosphate-Affinity PAGE Assay

Samples were resuspended in Phos-tag buffer (Wako Chemicals). To detect phosphorylated IF1, 30 μg of the sample was loaded in 10% polyacrylamide gels containing 80 μM Phos-tag acrylamide and 160 μM $MnCl_2$. Gels were transferred onto nitrocellulose membranes in the presence of 0.1 mM EDTA and further blotted against anti-IF1.

(C) Isolated mitochondria from HCT116 cells were incubated for 10 min with (+) or without (-) db-cAMP in the presence or absence of phosphatase inhibitors and IF1 identified on 2D gels.

(D) Hydrolase activity of the H^+-ATP synthase in isolated mitochondria from mouse heart. Where indicated, 30 μM OL (+OL) was added. A_{340}, absorbance at 340 nm.

(E) ATP production in isolated heart mitochondria.

(F and G) In (F), side views of the α (red)-, β (yellow)-, and γ (dark blue)-subunits of the bovine F1-ATPase and of its interaction with the 1–60 fragment of bovine IF1 (light blue) are shown. Images of the bovine F1-(I1-60His)$_2$ complex are taken from Bason et al. (2014) (PDB:4TSF), created with the PyMOL Molecular Graphics System. (G) Cross-sectional side view of the central stalk (dark blue) and the β-subunit (yellow) interacting with the IF1 fragment (light blue). The serine residue that is phosphorylated in the mature human IF1 (S14) is mapped and highlighted (red sphere) onto the bovine IF1 fragment. Note the close contact between S14 and the central stalk (dark blue).

(H) Signaling pathways (arrows) that convey on the activation of PKA (green) result in the phosphorylation of the bulk of IF1 (blue rods) present in the tissue. A broken arrow indicates the putative activity of a phosphatase on phosphorylated IF1. The phosphorylation of IF1 (orange/blue rods) prevents its interaction with the H^+-ATP synthase (yellow) and, hence, allows the synthesis of ATP. Dephosphorylated IF1 (blue rod) interacts with the H^+-ATP synthase and prevents the synthesis and hydrolysis of ATP. The fraction of dephosphorylated IF1 that is present in tissues with high energy demand triggers the inhibition of a fraction of the H^+-ATP synthase. Based on previous findings, we speculate that the IF1-mediated inhibition of the H^+-ATP synthase contributes to signaling mitohormesis.

Bars indicate mean ± SEM of four different mice per condition tested. *$p < 0.05$ when compared to CRL by Student's t test.

Statistical Analysis

Statistical analyses were performed using a two-tailed Student's t test. The results shown are means ± SEM. *p < 0.05 was considered statistically significant.

SUPPLEMENTAL INFORMATION

Supplemental Information includes Supplemental Experimental Procedures, two figures, and one table and can be found with this article online at http://dx.doi.org/10.1016/j.celrep.2015.08.052.

AUTHOR CONTRIBUTIONS

J.G.-B., M.S.-A., B.S., A.d.A., and C.N.-T. carried out experiments and analyzed data. J.G.-B. and M.S.-A. contributed in design of the paper. J.M.C. designed the study, carried out the analyses and interpretation of data, and wrote the manuscript. All authors read and approved the final manuscript.

ACKNOWLEDGMENTS

The technical assistance of M. Chamorro and C. Nunez de Arenas is acknowledged. J.G.-B. and C.N-T. were supported by pre-doctoral fellowships from FPI-MICINN/MINECO and Fondo Social Europeo, Spain. This work was supported by grants from Ministerio de Economía y Competitividad (SAF2013-41945-R), Comunidad de Madrid (S2011/BMD-2402), and Fundacion Ramon Areces (FRA), Spain. The CBMSO received an institutional grant from the FRA.

Received: April 16, 2015
Revised: July 28, 2015
Accepted: August 17, 2015
Published: September 17, 2015

REFERENCES

Acin-Perez, R., Salazar, E., Kamenetsky, M., Buck, J., Levin, L.R., and Manfredi, G. (2009). Cyclic AMP produced inside mitochondria regulates oxidative phosphorylation. Cell Metab. *9*, 265–276.

Acin-Perez, R., Gatti, D.L., Bai, Y., and Manfredi, G. (2011). Protein phosphorylation and prevention of cytochrome oxidase inhibition by ATP: coupled mechanisms of energy metabolism regulation. Cell Metab. *13*, 712–719.

Acín-Pérez, R., Carrascoso, I., Baixauli, F., Roche-Molina, M., Latorre-Pellicer, A., Fernández-Silva, P., Mittelbrunn, M., Sanchez-Madrid, F., Pérez-Martos, A., Lowell, C.A., et al. (2014). ROS-triggered phosphorylation of complex II by Fgr kinase regulates cellular adaptation to fuel use. Cell Metab. *19*, 1020–1033.

Bah, A., Vernon, R.M., Siddiqui, Z., Krzeminski, M., Muhandiram, R., Zhao, C., Sonenberg, N., Kay, L.E., and Forman-Kay, J.D. (2015). Folding of an intrinsically disordered protein by phosphorylation as a regulatory switch. Nature *519*, 106–109.

Bason, J.V., Montgomery, M.G., Leslie, A.G., and Walker, J.E. (2014). Pathway of binding of the intrinsically disordered mitochondrial inhibitor protein to F1-ATPase. Proc. Natl. Acad. Sci. USA *111*, 11305–11310.

Cabezon, E., Butler, P.J., Runswick, M.J., and Walker, J.E. (2000). Modulation of the oligomerization state of the bovine F1-ATPase inhibitor protein, IF1, by pH. J. Biol. Chem. *275*, 25460–25464.

Cabezón, E., Montgomery, M.G., Leslie, A.G., and Walker, J.E. (2003). The structure of bovine F1-ATPase in complex with its regulatory protein IF1. Nat. Struct. Biol. *10*, 744–750.

Campanella, M., Casswell, E., Chong, S., Farah, Z., Wieckowski, M.R., Abramov, A.Y., Tinker, A., and Duchen, M.R. (2008). Regulation of mitochondrial structure and function by the F1Fo-ATPase inhibitor protein, IF1. Cell Metab. *8*, 13–25.

Chen, Z., Odstrcil, E.A., Tu, B.P., and McKnight, S.L. (2007). Restriction of DNA replication to the reductive phase of the metabolic cycle protects genome integrity. Science *316*, 1916–1919.

Chen, W.W., Birsoy, K., Mihaylova, M.M., Snitkin, H., Stasinski, I., Yucel, B., Bayraktar, E.C., Carette, J.E., Clish, C.B., Brummelkamp, T.R., et al. (2014). Inhibition of ATPIF1 ameliorates severe mitochondrial respiratory chain dysfunction in mammalian cells. Cell Rep. *7*, 27–34.

Chin, R.M., Fu, X., Pai, M.Y., Vergnes, L., Hwang, H., Deng, G., Diep, S., Lomenick, B., Meli, V.S., Monsalve, G.C., et al. (2014). The metabolite α-ketoglutarate extends lifespan by inhibiting ATP synthase and TOR. Nature *510*, 397–401.

Christensen, G.L., Kelstrup, C.D., Lyngsø, C., Sarwar, U., Bøgebo, R., Sheikh, S.P., Gammeltoft, S., Olsen, J.V., and Hansen, J.L. (2010). Quantitative phosphoproteomics dissection of seven-transmembrane receptor signaling using full and biased agonists. Mol. Cell. Proteomics *9*, 1540–1553.

Christian, D.R., Kilsheimer, G.S., Pettett, G., Paradise, R., and Ashmore, J. (1969). Regulation of lipolysis in cardiac muscle: a system similar to the hormone-sensitive lipase of adipose tissue. Adv. Enzyme Regul. *7*, 71–82.

Danial, N.N., Gramm, C.F., Scorrano, L., Zhang, C.Y., Krauss, S., Ranger, A.M., Datta, S.R., Greenberg, M.E., Licklider, L.J., Lowell, B.B., et al. (2003). BAD and glucokinase reside in a mitochondrial complex that integrates glycolysis and apoptosis. Nature *424*, 952–956.

Di Benedetto, G., Scalzotto, E., Mongillo, M., and Pozzan, T. (2013). Mitochondrial Ca^{2+} uptake induces cyclic AMP generation in the matrix and modulates organelle ATP levels. Cell Metab. *17*, 965–975.

Di Benedetto, G., Pendin, D., Greotti, E., Pizzo, P., and Pozzan, T. (2014). Ca2+ and cAMP cross-talk in mitochondria. J. Physiol. *592*, 305–312.

Formentini, L., Sánchez-Aragó, M., Sánchez-Cenizo, L., and Cuezva, J.M. (2012). The mitochondrial ATPase inhibitory factor 1 triggers a ROS-mediated retrograde prosurvival and proliferative response. Mol. Cell *45*, 731–742.

Formentini, L., Pereira, M.P., Sánchez-Cenizo, L., Santacatterina, F., Lucas, J.J., Navarro, C., Martínez-Serrano, A., and Cuezva, J.M. (2014). In vivo inhibition of the mitochondrial H+-ATP synthase in neurons promotes metabolic preconditioning. EMBO J. *33*, 762–778.

Glancy, B., and Balaban, R.S. (2012). Role of mitochondrial Ca2+ in the regulation of cellular energetics. Biochemistry *51*, 2959–2973.

Gledhill, J.R., Montgomery, M.G., Leslie, A.G., and Walker, J.E. (2007). How the regulatory protein, IF(1), inhibits F(1)-ATPase from bovine mitochondria. Proc. Natl. Acad. Sci. USA *104*, 15671–15676.

Gordon-Smith, D.J., Carbajo, R.J., Yang, J.C., Videler, H., Runswick, M.J., Walker, J.E., and Neuhaus, D. (2001). Solution structure of a C-terminal coiled-coil domain from bovine IF(1): the inhibitor protein of F(1) ATPase. J. Mol. Biol. *308*, 325–339.

Huang, L.J., Durick, K., Weiner, J.A., Chun, J., and Taylor, S.S. (1997). D-AKAP2, a novel protein kinase A anchoring protein with a putative RGS domain. Proc. Natl. Acad. Sci. USA *94*, 11184–11189.

Kamp, T.J., and Hell, J.W. (2000). Regulation of cardiac L-type calcium channels by protein kinase A and protein kinase C. Circ. Res. *87*, 1095–1102.

Kinoshita, E., Kinoshita-Kikuta, E., and Koike, T. (2009). Separation and detection of large phosphoproteins using Phos-tag SDS-PAGE. Nat. Protoc. *4*, 1513–1521.

Livigni, A., Scorziello, A., Agnese, S., Adornetto, A., Carlucci, A., Garbi, C., Castaldo, I., Annunziato, L., Avvedimento, E.V., and Feliciello, A. (2006). Mitochondrial AKAP121 links cAMP and src signaling to oxidative metabolism. Mol. Biol. Cell *17*, 263–271.

Means, C.K., Lygren, B., Langeberg, L.K., Jain, A., Dixon, R.E., Vega, A.L., Gold, M.G., Petrosyan, S., Taylor, S.S., Murphy, A.N., et al. (2011). An entirely specific type I A-kinase anchoring protein that can sequester two molecules of protein kinase A at mitochondria. Proc. Natl. Acad. Sci. USA *108*, E1227–E1235.

Mourier, A., Ruzzenente, B., Brandt, T., Kühlbrandt, W., and Larsson, N.G. (2014). Loss of LRPPRC causes ATP synthase deficiency. Hum. Mol. Genet. *23*, 2580–2592.

Pagliarini, D.J., and Dixon, J.E. (2006). Mitochondrial modulation: reversible phosphorylation takes center stage? Trends Biochem. Sci. *31*, 26–34.

Papa, S., De Rasmo, D., Scacco, S., Signorile, A., Technikova-Dobrova, Z., Palmisano, G., Sardanelli, A.M., Papa, F., Panelli, D., Scaringi, R., and

Santeramo, A. (2008). Mammalian complex I: a regulable and vulnerable pacemaker in mitochondrial respiratory function. Biochim. Biophys. Acta *1777*, 719–728.

Paumard, P., Vaillier, J., Coulary, B., Schaeffer, J., Soubannier, V., Mueller, D.M., Brèthes, D., di Rago, J.P., and Velours, J. (2002). The ATP synthase is involved in generating mitochondrial cristae morphology. EMBO J. *21*, 221–230.

Rizzuto, R., De Stefani, D., Raffaello, A., and Mammucari, C. (2012). Mitochondria as sensors and regulators of calcium signalling. Nat. Rev. Mol. Cell Biol. *13*, 566–578.

Sánchez-Aragó, M., Chamorro, M., and Cuezva, J.M. (2010). Selection of cancer cells with repressed mitochondria triggers colon cancer progression. Carcinogenesis *31*, 567–576.

Sánchez-Aragó, M., Formentini, L., and Cuezva, J.M. (2013a). Mitochondria-mediated energy adaption in cancer: the H(+)-ATP synthase-geared switch of metabolism in human tumors. Antioxid. Redox Signal. *19*, 285–298.

Sánchez-Aragó, M., Formentini, L., Martínez-Reyes, I., García-Bermudez, J., Santacatterina, F., Sánchez-Cenizo, L., Willers, I.M., Aldea, M., Nájera, L., Juarránz, A., et al. (2013b). Expression, regulation and clinical relevance of the ATPase inhibitory factor 1 in human cancers. Oncogenesis *2*, e46.

Sánchez-Aragó, M., García-Bermúdez, J., Martínez-Reyes, I., Santacatterina, F., and Cuezva, J.M. (2013c). Degradation of IF1 controls energy metabolism during osteogenic differentiation of stem cells. EMBO Rep. *14*, 638–644.

Sánchez-Cenizo, L., Formentini, L., Aldea, M., Ortega, A.D., García-Huerta, P., Sánchez-Aragó, M., and Cuezva, J.M. (2010). Up-regulation of the ATPase inhibitory factor 1 (IF1) of the mitochondrial H+-ATP synthase in human tumors mediates the metabolic shift of cancer cells to a Warburg phenotype. J. Biol. Chem. *285*, 25308–25313.

Schaar, C.E., Dues, D.J., Spielbauer, K.K., Machiela, E., Cooper, J.F., Senchuk, M., Hekimi, S., and Van Raamsdonk, J.M. (2015). Mitochondrial and cytoplasmic ROS have opposing effects on lifespan. PLoS Genet. *11*, e1004972.

Sharma, K., D'Souza, R.C., Tyanova, S., Schaab, C., Wiśniewski, J.R., Cox, J., and Mann, M. (2014). Ultradeep human phosphoproteome reveals a distinct regulatory nature of Tyr and Ser/Thr-based signaling. Cell Rep. *8*, 1583–1594.

Steinberg, S.F., and Brunton, L.L. (2001). Compartmentation of G protein-coupled signaling pathways in cardiac myocytes. Annu. Rev. Pharmacol. Toxicol. *41*, 751–773.

Valsecchi, F., Ramos-Espiritu, L.S., Buck, J., Levin, L.R., and Manfredi, G. (2013). cAMP and mitochondria. Physiology (Bethesda) *28*, 199–209.

Vives-Bauza, C., Yang, L., and Manfredi, G. (2007). Assay of mitochondrial ATP synthesis in animal cells and tissues. Methods Cell Biol. *80*, 155–171.

Walker, J.E. (2013). The ATP synthase: the understood, the uncertain and the unknown. Biochem. Soc. Trans. *41*, 1–16.

Wright, P.E., and Dyson, H.J. (2015). Intrinsically disordered proteins in cellular signalling and regulation. Nat. Rev. Mol. Cell Biol. *16*, 18–29.

Yun, J., and Finkel, T. (2014). Mitohormesis. Cell Metab. *19*, 757–766.

Zhao, X., León, I.R., Bak, S., Mogensen, M., Wrzesinski, K., Højlund, K., and Jensen, O.N. (2011). Phosphoproteome analysis of functional mitochondria isolated from resting human muscle reveals extensive phosphorylation of inner membrane protein complexes and enzymes. Mol. Cell Proteomics *10*, M110.000299.

Zhou, H., Di Palma, S., Preisinger, C., Peng, M., Polat, A.N., Heck, A.J., and Mohammed, S. (2013). Toward a comprehensive characterization of a human cancer cell phosphoproteome. J. Proteome Res. *12*, 260–271.